Short-range Forecasting Research

Short Range Forecasting Division

Technical Report No.12

Detection of Precipitation by Radars in the UK Weather Radar Network

by

M. Kitchen and P.M. Brown

April 1992

Meteorological Office
London Road
Bracknell
Berkshire
RG12 2SZ
United Kingdom

Detection of Precipitation by Radars in the UK Weather Radar Network

by

M Kitchen and P M Brown

April 1992

S Division Technical Report No. 12

Short Period Forecasting Research Division
Meteorological Office
London Road
Bracknell
Berks, RG12 2SZ

Note

DETECTION OF PRECIPITATION BY RADARS IN THE UK WEATHER RADAR NETWORK

M Kitchen and P M Brown
Meteorological Office, Bracknell, U.K.

Abstract

The long-term performance of radars in the United Kingdom operational weather radar network was simulated using reflectivity profiles measured by the high resolution Chilbolton research radar. Comparisons between the results of these simulations and operational data suggested that the probability of detection is rather worse than would be predicted from consideration of the radar specification. The cause of this discrepancy was investigated by direct comparison between the Chilbolton and Chenies radars. The effective detection threshold of the Chenies radar was estimated to be as high as $\approx 0.5mmh^{-1}$ at a range of 111km, compared with the specification of $\leq 0.14mmh^{-1}$. As an illustration of the seriousness of the problem, the radar is only able to detect rain at 200km range in winter on about 6% of the occasions that it should be able to. There is evidence that most other radars in the network suffer from similar detection problems, although to a lesser extent.

1 Introduction.

Previous work by Carpenter (1985) and Brown (1987) in which rainfall data from radars in the United Kingdom (UK) weather radar network were compared with synoptic observations of rain, suggested rather low probabilities of detection (POD). Even with drizzle excluded, POD was typically ≈ 0.7 close to the radars and ≈ 0.3 or less at ranges above about 150km. Carpenter concluded that the detection problem was the main factor limiting the quality of the rainfall analysis, although sampling differences may have been responsible for some apparent detection failures. Unfortunately, this type of comparison was unable to identify the cause of the low detection rates.

Range corrections are applied to the radar data to compensate for the effects of incomplete beam filling and the fall off in reflectivity above the melting layer. The importance of range effects has recently been emphasised by Joss and Waldvogel (1990) and Smith (1990) and there has been some quantitative work on corrections by e.g. Koistinen (1991), Tees and Austin (1991) and by Brown et al (1987). These correction schemes are designed to achieve the best analysis of instantaneous rainfall rate and cannot compensate for missing rain. However, in hydrological applications of radar data, areal average accumulations over catchments are often required rather than instantaneous rates. For these purposes, it is particularly important to know if significant precipitation is not being detected.

Apart from the work by Brown and Carpenter, the subject of precipitation detection appears to have escaped attention in the literature. The purpose of this work was therefore to quantify the POD for the benefit of users of UK radar network data. Also, if the low POD values reported previously were confirmed, to investigate the cause.

Comparisons between radar and gauges or synoptic observations are subject to large uncertainty due to temporal and spatial sampling differences. The interpretation of results from the previous studies by Carpenter and Brown has been open to some doubt as a result. To overcome such problems, the approach adopted here was to obtain a large dataset of high resolution vertical profiles of reflectivity which could be used to simulate the measurements from operational radars.

Two types of simulation experiment were performed. Firstly, large sets of reflectivity profiles were used to simulate overall and seasonal radar performance. Statistics summarising the results of these simulations were then compared with similar qauntities derived from long-term integrations of operational radar data. To assist in the interpretation of the results, some direct comparisons were made between reflectivities measured by the Chenies operational radar and simulations based upon collocated Chilbolton reflectivity profiles.

2 High vertical resolution reflectivity profiles.

The high resolution reflectivity profiles were obtained from the 10cm wavelength Chilbolton radar operated by the Rutherford Appleton Laboratory. The radar is located near Andover in southern England at a height of 92m above mean sea level (AMSL). These data were collected on a regular basis for 9 days in every 28 over the two year period autumn 1987 to autumn 1989. Data were not recorded if there was no precipitation falling within the scanned area and dataset contains recordings from a total of 112 'wet' days. The radar executed series of 3 RHI scans along azimuths to the SW of Chilbolton, above topography typical of southern England (see Fig 1).

If measurements from the operational weather radars are to be simulated accurately from reflectivity profile data, it is essential that the profiles have a higher vertical resolution than the beamwidth of the operational radar measurements. This requirement is fulfilled as the Chilbolton radar half-power beamwidth is only 0.25 deg compared to 1.0 deg for the operational radars. The reflectivity profiles were generated from RHI scans where the elevation angle was stepped in intervals of 0.25 deg from 0-15 deg and the resolution of the data in range was $\simeq 300m$. As data from the operational radars are used out to ranges where the radar beam is centred up to about 5km AMSL, it was required that the reflectivity profiles used in the simulation experiment must contain data at least up to this level. To obtain the best compromise between vertical resolution and height range, RHI data within the range band 20-36km were used. At 20km range, the highest elevation ray is centred at a height of 5.4km AMSL.

Basic data from the Chilbolton radar are produced by averaging the absolute magnitude of the received signals. This procedure avoids the large sampling errors which can be introduced by averaging the logarithmic amplitude (see Seed and Austin, 1990). The signal processing for the operational radars is similar, except that when data on a 1 deg x 1.5km polar grid (sample area $\simeq 1.5 \times 0.5km \equiv 0.75km^2$ at 30km range) are averaged to give data on a 5 x 5km cartesian grid, the reflectivity values are first transformed to equivalent rainfall rate.

Some thought was given to the best method of constructing average reflectivity profiles from

the Chilbolton data which would be characteristic of the 5km pixels used in the operational radar analysis. At 30km range, the half-power beam width of the Chilbolton beam is only $\simeq 0.13km$ so the RHI data represents essentially a line sample across an area 5x5 km. The average length of a line sample crossing a 5km pixel through its centre is 5.6km. Thus to achieve approximately the correct linear scale, reflectivity measurements from 18 adjacent 0.3km range gates within an RHI scan were grouped according to the height of the sample volume AMSL and the average reflectivity within height intervals 200m deep computed. It was then assumed that the average reflectivity along this line sample within a height bin was the same as over a 5km pixel.

Each RHI scan occupied about 30 seconds and the scan sequence was repeated at intervals of 10 minutes. Three reflectivity profiles were derived from each Chilbolton RHI scan and the total number of profiles in the dataset was $\approx$ 14400. The large number of profiles and random method of selecting days on which to record data was necessary to ensure that the profiles are representative of all conditions. To avoid problems with beam occultation and ground clutter at low elevation angles, radar data from levels below 400m AMSL were not used. If the reflectivity in the layer centred at 500m was less than $5mm^6m^{-3}$, the profile was excluded from the analysis. In conditions favourable for the growth of precipitation by the Bergeron seeder-feeder mechanism, precipitation growth below 400m may be significant over topography similar to that around Chilbolton (see Kitchen and Blackall 1992). Except in cases of orographic growth, there is no evidence of systematic gradients in reflectivity in the lowest few hundred metres above the ground (see e.g. Harper ,1957). Therefore a constant reflectivity was assumed below 400m AMSL. This assumption of may result in some uncertainties in the simulation of radar operational radar performance at shorter ranges. A longer ranges, the operational radar beam used is at an elevation angle of 0.5 degrees for all but one of the radars. The beam centre is at $> 1km$ AMSL for ranges beyond about 80km and the reflectivity measurements will be relatively insensitive to variations in reflectivity in the lowest 400m. The reflectivity measurement in the height band centred at $\simeq 500m$ AMSL defined the equivalent rainfall rate R_0. R_0 is subsequently referred to as the surface rainfall rate, although note that if the melting layer is within a few hundred metres of the surface, R_0 may seriously overestimate the true surface rainfall rate.

For the direct comparisons between Chilbolton and Chenies radars, Chilbolton reflectivity data within a single 5km pixel in the area of Chenies radar coverage were averaged to provide a vertical reflectivity profile. The pixel was located at a range of 111km from the Chenies radar and 25km from Chilbolton (see Fig 1). This pixel was chosen to be in a low-lying area to minimise any gradients in the profile due to orographic growth.

3 Simulation of operational radar measurements.

The measured reflectivity ($\overline{Z}$) is obtained from the vertical reflectivity profiles using the following equations (from Brown et al, 1989).

$$\overline{Z} = \int_{\alpha}^{\beta} Z(\phi) f(\phi) d\phi \tag{1}$$

where ϕ is the elevation angle, $f(\phi)$ is the fraction of the radar beam power in the range ϕ to $\phi + d\phi$ and the beam power is negligible outside the range of angles α to β.

$$f(\phi)d\phi = [P(\phi)d\phi] / \int_{\alpha}^{\beta} P(\phi)d\phi \quad (2)$$

and $P(\phi)d\phi$ is the relative power returned from angles in the range ϕ to $\phi + d\phi$. The transmitted beam power profile relative to the beam centre ($\phi = 0$) specified by the radar manufacturers is well fitted by the function $[\sin(k\phi)/k\phi]^2$, where k is a constant (=159.46 for ϕ in degrees). The function falls to zero for $|\phi| > 1.13$ degrees and the power is assumed to be zero outside this range. The half-power beam width is 1 degree. Therefore the received power profile is given by:-

$$P(\phi) = [\sin(k\phi)/k\phi]^4 \quad (3)$$

Values of $\overline{Z}$ at 8 values of radar range from 25-200km were found by integration of equation 1 using 0.01 degree angular increments. Refraction of the radar beam was taken into account using the ' 4/3rds earth' correction. For the operational radars, the minimum acceptable signal in an individual 1 deg x 187.5m polar cell is set at a value of $\overline{Z}$ equivalent to a rainfall rate of $0.125mmh^{-1}$ at a range of 100km ($\equiv 7.2mm^6m^{-3}$). If a single polar cell within a 5km pixel has a measured reflectivity above the threshold, and the average reflectivity over the pixel is equivalent to a rainfall rate $> 0.031mmh^{-1}$, then the radar should record precipitation. The effective detection threshold, (denoted by Z_T) was taken to be the higher figure, $7.2mm^6m^{-3}$, in this analysis. Note that this should give a rather pessimistic view of the radars ability to detect precipitation.

At ranges $< 100km$, range dependent attenuation of the received signals is applied and the limit is therefore constant over this range. For ranges $> 100km$, the detection limit will increase with the square of the range, i.e. $Z_T(r > 100km) = (r^2/100^2)Z_T(r = 100)$ The sensitivity of the Chilbolton radar is determined by a minimum signal output of 4dB $\equiv 2.5mm^6m^{-3}$ for ranges up to 110km. It is impossible, from the available data, to simulate precisely the processing and averaging of the raw radar signals which fluctuate in space and time. Thus, given a reflectivity profile measured by the Chilbolton radar, no categorical statement can be made as to whether an operational radar would or would not have been able to detect precipitation. The simplest assumption was made that if the estimate of the reflectivity that would be measured by an operational radar at a given range fell below Z_T, the radar was judged not to be able to detect the precipitation. Throughout the radar data processing and data analysis, where reflectivity has been converted to equivalent rainfall rate, a Z-R relationship of the form $Z = 200.R^{1.6}$ was assumed.

To demonstrate the relative importance of detection failures and rainfall rate underestimation, three statistics were derived from the results of the simulation experiment:-

$\Sigma R(\overline{Z} > Z_T)/\Sigma R_0$, the ratio of the measured accumulation to the surface accumulation;
$N(\overline{Z} > Z_T)/N$, the probability of detection;
$(\Sigma R(\overline{Z} > Z_T)/N(\overline{Z} > Z_T))/(\Sigma R_0/N)$, the ratio of the average measured rainfall rate (excluding detection failures) to the average rate at the surface.

The three quantities are related by the equation:-

$$\Sigma R(\overline{Z} > Z_T)/\Sigma R_0 = N(\overline{Z} > Z_T)/N \times (\Sigma R(\overline{Z} > Z_T)/N(\overline{Z} > Z_T))/(\Sigma R_0/N) \quad (4)$$

where the normalised accumulation on the LHS is decomposed into two terms; the first term on the RHS is the contribution from detection failures and the second term is the effect of rate underestimation. All three terms being unity would represent perfect performance.

Fig 2 shows the three terms plotted as a function of range for a radar sited 100m AMSL with a beam elevation of 0.5 degrees. Simulations based upon the entire profile dataset (Fig 2a) indicate that the measured rainfall accumulation at a range of 200km is about one quarter of the surface value. At ranges up to about 110km, the tendency is for the radar to overestimate surface accumulations due to enhanced reflectivity in the melting layer. The probability of detection declines steadily with range down to 0.41 at 200km and is the dominant factor in the range performance.

In winter, the effect of range on measured accumulations is much larger, with the measured accumulation being less than 0.1 of the surface value at 200km (Fig 2b). Also, the contribution from detection failures and measured rainfall rates is comparable at longer ranges. Radar overestimation of surface rainfall on average is confined to ranges less than about 80km because of the lower average height of the melting layer in winter. In summer, the range performance is rather better, with the average measured rainfall rate tending to increase with range, reflecting the higher average height of the melting layer and depth of precipitation. Nevertheless, the measured accumulations decrease with range beyond 125km due to the decreasing probability of detection.

4 Operational radar performance revealed by long-term integration of data

If radar data are integrated over a sufficiently long period, then spatial variations in rainfall over the area covered by a single radar (maximum range 210km) should be largely smoothed out. Some systematic variations due to e.g. orographic enhancement, beam occultation and ground clutter may remain, but averaging in azimuth should reduce such variations. Similarly, geographical variations due to e.g. a general east-west gradient across the UK, may result in differences in average rainfall rates and accumulations between radars. However long-term integrations should be able to provide information on the relative performance of the radars as a function of range.

Rainfall rate measurements over a single wet month (February 1990) from each of the operational radars were grouped according to the pixel range from the radar. The radar data were at intervals of 15 minutes and $\approx$ 2500 instantaneous rainfall rate fields from each radar were analysed. The effect of gauge adjustment and empirical range corrections (over and above the usual inverse square correction) was reversed to leave 'raw' data, but the attenuation correction was retained. Only pixels covered by the lowest elevation beam (0.5 deg elevation for all radars except 0.0 deg for Clee) were included in the analysis. Data from higher elevation beams is mainly used close to the radar to minimise ground clutter and occultation effects.

Let the number of pixels in each 10km range band multiplied by the number of analysed images be n, and the corresponding number of 'wet' pixel cases be $n(R > 0)$. Three quantities were computed for each range band; the mean rainfall rate, $(1/n)\Sigma R$ (which is proportional to the accumulation per pixel); the frequency of rain in each pixel, $n(R > 0)/n$ (proportional to the POD); and the mean rainfall rate for 'wet' pixels, $(1/n(R > 0)\Sigma R$. These quantities are analogous to the three terms in equation 4, although they are not normalised in the same way because the surface rainfall

is unknown. They are related through the equation;

$$(1/n)\Sigma R = n(R > 0)/n \times (1/n(R > 0)\Sigma R \tag{5}$$

The variation in these quantities as a function of range for 8 radars in the operational network is shown in Fig 3.

The curves for the different radars show large variations in shape at shorter ranges, with several radars showing marked peaks in the measured rainfall rate at ranges between 50 and 100km; presumably due to the bright band. Some of the differences between the curves may also be due to variable amounts of clutter and orographic rainfall. At ranges $> 100km$, where the effect of range causes a general decrease in the measured rainfall rates and the POD, the curves are much smoother. The Chenies and Lincoln radars recorded some of the lowest average rainfall rates in Fig 3a, and as both radars are in Eastern England, this may be evidence of regional variations in rainfall during this month. In view of this lack of normalization, it is appropriate to to compare the ratios between values at different ranges rather than the absolute magnitude of the values plotted in Fig 3. This had the additional benefit of allowing direct comparison with the results from the simulation experiments plotted in Fig 2b. The key assumption in the latter comparison is that the distribution of precipitation profiles within each radar area in February 1990 was not significantly different from the distribution for the winter months in the Chilbolton profile dataset.

The ratio $(n(R > 0)/n)_{200}/(n(R > 0)/n)_{100}$, where the subscripts refer to range in km, was chosen as a measure of the rate of decrease of POD at longer ranges and may be directly compared with the ratio $N(\overline{Z} > Z_T)_{200}/N(\overline{Z} > Z_T)_{100}$ from the simulation experiments. These ratios are plotted as a function of radar antenna height in Fig 4a. Of the 8 operational radars for which the detection rates have been evaluated, only Predannack and Wardon Hill, have ratios which are higher than the results of simulations based on the conservative estimate of the detection threshold. Although Clee radar provided the next highest value of $(n(R > 0)/n)_{200}/(n(R > 0)/n)_{100} = 0.19$, a simulation suggested that the ratio should be at least 0.63 for this radar with its 0.0 deg elevation beam. The Chenies radar showed the most rapid decline in relative detection frequency by a considerable margin. Castor Bay, Lincoln, Dyfed and Hameldon all show a more rapid fall off in detection with range than anticipated which is indicative of problems similar to, but perhaps not as serious as, that at Chenies. The ratio $(n(R > 0)/n)_{200}/(n(R > 0)/n)_{100}$ was also expected to vary smoothly with the height of the radar antenna. That this was not the case provides further evidence of unexplained differences between radars.

The two radars which showed the highest detection rates also appear to have been the most sensitive, with higher average rainfall rates in 'wet' pixels for most ranges (Fig 3c). Chenies and Clee radars showed the lowest relative decline in average rainfall rate with range i.e. the highest values of the ratio $(\Sigma R/n(R > 0))_{200}/(\Sigma R/n(R > 0))_{100})$ in Fig 4b. This is symptomatic of a failure to detect the lower reflectivities at long range. More conclusive evidence of a specific problem with the Chenies radar is provided in the next section.

The ratios plotted in Fig 4b are almost all higher than those plotted in Fig 4a. This shows that the decrease in rainfall accumulations from most radars at ranges beyond 100km (evidenced by Fig 3a) is mainly as a result of the decline in the frequency of detection.

There are some other features of the curves plotted in Fig 3 which merit further investigation and it is anticipated that these will form the subject of a further report.

5 Direct comparison between Chilbolton and Chenies radars

To investigate the causes of the discrepancy between POD results from the simulations and the integrations of operational data, some direct comparisons were made between the Chilbolton and Chenies radars. Cases selected were mainly of frontal rainfall to minimise scatter due to spatial variations in rainfall across the comparison pixel. Chenies data recorded at the radar site were utilised because data are available from different beam elevations with a 5 minute sampling interval. In each case, the measurements from the Chenies beams at elevation angles of 0.5, 1.5 and 2.5 degrees were simulated using the reflectivity profile constructed from Chilbolton RHI data within the pixel. The comparison pixel lay along azimuth 228 degrees from Chenies and in this direction, the radar horizon is below 0 deg. Thus occultation effects were not likely to be important and were not considered in the simulations. Examples of time series of the simulated measurements and actual Chenies measurements are shown in Fig 5. Simulated rainfall rates > 0 were then compared with interpolations from the Chenies measurement series. A comparison was rejected if there was no Chenies measurement within 5 minutes of the Chilbolton data time or the two Chenies measurements used in the interpolation were separated by more than 15 minutes. Scatter plots are shown for different cases and different beam elevations in Fig 6 a)-d). Random differences may be expected to arise from the temporal interpolation or differences between the reflectivity profile derived from the Chilbolton RHI scan through the pixel and the true areal average profile over the pixel. However, the scatter is sufficiently small to allow a reasonable determination of the intercept on the Y-axis. The method of least squares using only points with $0 < R < 5mmh^{-1}$ was used for this purpose, although note that a straight line may not be the best fit to the comparison data. The intercepts lay in the range range $0.18 - 0.80mmh^{-1}$ i.e. all were above the upper limit from the radar specification (Table 1). These estimates are supported by the many points lying along the Y-axis, i.e. comparisons with simulated values of $R > 0$ and the measured $R = 0$. The weighted mean of the intercept estimates in Table 1 was $0.5mmh^{-1}$. This should be compared with the Chenies radar specification which implies a detection threshold of no higher than $0.125mmh^{-1}$ for ranges $< 100km$ and $\leq 0.14mmh^{-1}$ in the comparison pixel at 111km range.

To show the effect of such a high detection threshold upon operational radar performance, Chenies performance in winter was simulated using both the specification threshold value and our best estimate of the effective threshold for the Chenies radar ($Z_T = 66mm^6m^{-3} \equiv 0.5mmh^{-1}$ at a range of 111km). Out of the three terms in equation 4, the largest effect of the increased threshold is upon the probability of detection (Fig 7). At 150km range, the radar is only able to detect rainfall on about half of the occasions it should be able to; at 200km, the fraction is only 0.06.

Values of $N(\overline{Z} > Z_T)_{200}/N(\overline{Z} > Z_T)_{100}$, assuming the high detection threshold, were added to Fig 4 for comparison. The agreement with the measured ratio for Chenies is to be expected, given that the value of the threshold was derived from the results of similar simulations.

From Fig 7b, an increase in the threshold from 0.125 to $0.44mmh^{-1}$ results in a decrease of POD of about 30% at a range of 25km. It is possible to confirm this reduction independently if we assume that the radar beam is typically intercepting rain below the cloud base at this range. Breuer and Kreuels (1977) published rainfall rate distributions measured by a disdrometer at Bonn, Germany. Assuming the Taylor hypothesis applies to rainfall rate and the characteristic advection velocity is of order $10ms^{-1}$, variations in instantaneous rainfall rate on a horizontal scale of 5km should be roughly equivalent to variations at a point averaged over periods of order 500 seconds. Breuer

and Kreuels tabulated distributions for integration periods of 300 and 600 seconds. The percentage duration of rainfall $> 0.2mmh^{-1}$ in the range $0.2 - 0.5mmh^{-1}$ was 44% in both, which confirms that the Chenies radar will significantly underestimate the frequency of precipitation, even at short range. The meteorological definition of 'slight rain' is a rate of $< 0.5mmh^{-1}$ (Meteorological Office, 1956), so most rainfall in this category will be missed by the Chenies radar unless the reflectivity is enhanced within the melting layer.

The impact of changes in the detection threshold upon measured accumulations and rainfall rates is less certain as further assumptions are necessary concerning the form of the relationship between the true and measured reflectivities. For example, the dashed lines in Figs 7a and 7c are based upon the assumption that the Chenies measurements are accurate for all $\overline{Z} > Z_T$.

In view of the important implications of these results, possible physical causes for the discrepancy in detection threshold were considered.

The Chenies and Chilbolton radars operate at different wavelengths (5.6 and 10cm respectively). This could possibly introduce some differences in scattering from very large aggregated hydrometeors in the melting layer. It could be expected that differences in beam heights and case-to-case variations in the height of the melting layer would ensure that only a fraction of the comparisons were affected. Thus the consistency in the intercept estimates in Table 1 would appear to rule this out as a significant effect.

There will be some uncertainty in the Chenies measurements due to imperfections in the attenuation corrections. The two-way attenuation (in $dBkm^{-1}(mmh^{-1})^{-1}$) at 5.6cm wavelength due to rain is approximated by $0.0044R^{0.31}$ (Gunn and East, 1954). If we assume that the maximum attenuation would be that due to say $R = 4mmh^{-1}$ over the entire 111km path length, then this would result in attenuation of 2.5dB, equivalent to a fractional decrease in rainfall rate to 0.7 of the uncorrected value. Thus attenuation results in only small reductions in the estimated detection threshold and it seems improbable that errors in the attenuation correction could explain the detection failures.

The assumed Chenies beam profile used in the simulation experiments may be different from the real profile. Occultation is not expected to be significant given the low radar horizon in the relevant direction. The fact that the beams at different elevation angles do not result in systematically different values of the intercept (see Table 1) is evidence that this is the case. If the bottom of the beams were occluded, the lowest elevation beam would be subject to the worst detection problems. For anomalous refraction to result in Chenies detection failures, the Chenies beam would have to be bent upwards significantly (refraction normally results in the beam being towards the ground). Such unusual atmospheric profiles could not persist over all the case studies.

There will be some uncertainty in the the threshold estimates arising from errors in the Chilbolton radar calibration. However, the slopes listed in Table 1 show that in most of the comparisons, the Chilbolton radar was reading lower than Chenies and the intercept was independent of the slope. There is no evidence of significant overestimation by the Chilbolton radar.

Having excluded as far as possible the alternative explanations, we are left with the possibility that there is a fault in the Chenies radar. The results of the analysis of operational data presented in Figs 3 and 4 represent strong evidence in support of this conclusion.

6 Conclusions

Comparisons between Chilbolton and Chenies radars suggest that the effective detection threshold of the Chenies radar is significantly higher than the radar specification would suggest. The best estimate of the threshold is $\simeq 0.5mmh^{-1}$ at a range of 111km. Radar performance at all ranges is affected, but the problem is more serious at long range. Further comparisons and examination of the raw polar data may provide further insight into the problem.

Analysis of data from eight operational radars has revealed that similar detection problems, although not as serious, affect all but two of the newer radars.

A pronounced range effect is evident in operational radar data. The steep decline in probability of detection at long range causes a similar fall off in measured rainfall accumulations. For ranges $> 100km$, the contribution from radar underestimation of precipitation rate is relatively smaller.

Simulations based upon the Chilbolton data suggest that if the radar detection threshold could be lowered to the specification value, radar performance would be much improved, particularly at long range. Nevertheless, failures in detection would still be the main cause of a decrease in measured accumulations beyond 100km range.

The simulations indicate marked seasonal differences in range performance. In winter, for a radar 100m AMSL working normally, detection failures and rainfall underestimation make roughly equal contributions to the the decline in measured accumulations at ranges $> 100km$. In summer, there is no overall underestimation at long range, but declining POD causes a decrease in measured accumulations beyond 150km range. At 200km range, the POD in winter would be about 0.25 compared to 0.44 in summer.

Hydrological applications of radar data require analyses and forecasts of areal average accumulations over catchments. Given the importance of detection failures and their effect upon measured accumulations, users need to be advised of the circumstances in which accumulations are likely to be significant underestimates.

7 Acknowledgements

John Goddard and Kevin Morgan of the Rutherford Appleton Laboratory provided advice on the processing of the Chilbolton radar data. The Chenies data tapes used in the direct comparison experiment were supplied by the Operational Instrumentation branch.

8 References.

Breuer L J and Kreuels R K 1977 Rainfall drop spectra intensities and fine structures on different time bases. Ann. Telecommunic. 32 p430-436

Brown R 1987 The variation in the probability of detection with range from comparisons with synoptic observations. Unpublished Nowcasting Research Group Report No 14, Meteorological Office.

Brown R, Sargent G P and Blackall R M 1991 Range and orographic corrections for use in real-time radar data analysis. Hydrological applications of weather radar. eds I D Cluckie and C G Collier, published by Ellis Horwood, Chichester. p 219-228.

Carpenter K M 1985 Assessing the impact of FRONTIERS on radar derived rainfall fields. Unpublished FRG Report No 90, Meteorological Office.

Gunn K L S and East T W R 1954 The microwave properties of precipitation particles. Q J R Met. Soc. 80 p522-545

Harper W G 1957 Variation with height of rainfall below the melting level. Q J R Met Soc. 83 p 368-371

Joss J and Waldvogel A 1990 Precipitation measurements and hydrology. Radar in meteorology, ed. D Atlas. Batten Memorial and 40th radar meteorology conference. Published by American Met. Soc. p577-606.

Kitchen M and Blackall R M 1992 Orographic rainfall over low hills and associated corrections to radar measurements. To appear in the Journal of Hydrology.

Koistinen J 1991 Operational correction of radar rainfall errors due to the vertical reflectivity profile. Proc. AMS 25th Int Conf on Radar Meteorology Paris. p91-94

Meteorological 1956 Observers Handbook. Meteorological Office

Office publication No M.O.554 221pp.

Seed A and Austin G L 1990 Variability of summer Florida rainfall and its significance for the estimation of rainfall by gages, radar and satellite. Journal of Geophysical Res. 95 p2207-2215.

Smith P L 1990 Precipitation measurement and hydrology: Panel Report. Radar in meteorology, ed. D Atlas. Batten Memorial and 40th radar meteorology conference. Published by American Met. Soc. p607-618.

Tees D and Austin G L 1989 The effect of range on the radar measurement of rainfall. Hydrological Applications of Weather Radar, eds I D Cluckie and C G Collier. Published by Ellis Horwood, Chichester. p298-304.

Table 1

Least squares estimates of Chenies radar detection threshold

Case	Beam elevation (degrees)	Slope	Intercept (mm/h)	Standard error in intercept (mm/h)
9/10 Oct 87	0.5	2.55	0.52	0.36
9/10 Oct 87	1.5	2.54	0.59	0.19
11 Nov 87	0.5	0.49*	0.77	0.57
28 Sep 88	1.5	2.09	0.18	0.46
18 Oct 88	1.5	0.70	0.80	0.62
18 Oct 88	2.5	0.47	0.56	0.26
19/20 Oct 89	0.5	0.43*	0.51	0.28
19/20 Oct 89	1.5	0.64	0.42	0.20
19/20 Oct 89	2.5	0.73	0.31	0.39
Best estimate of intercept (weighted mean)			0.50	

* Slope may have been modified by gauge adjustment.

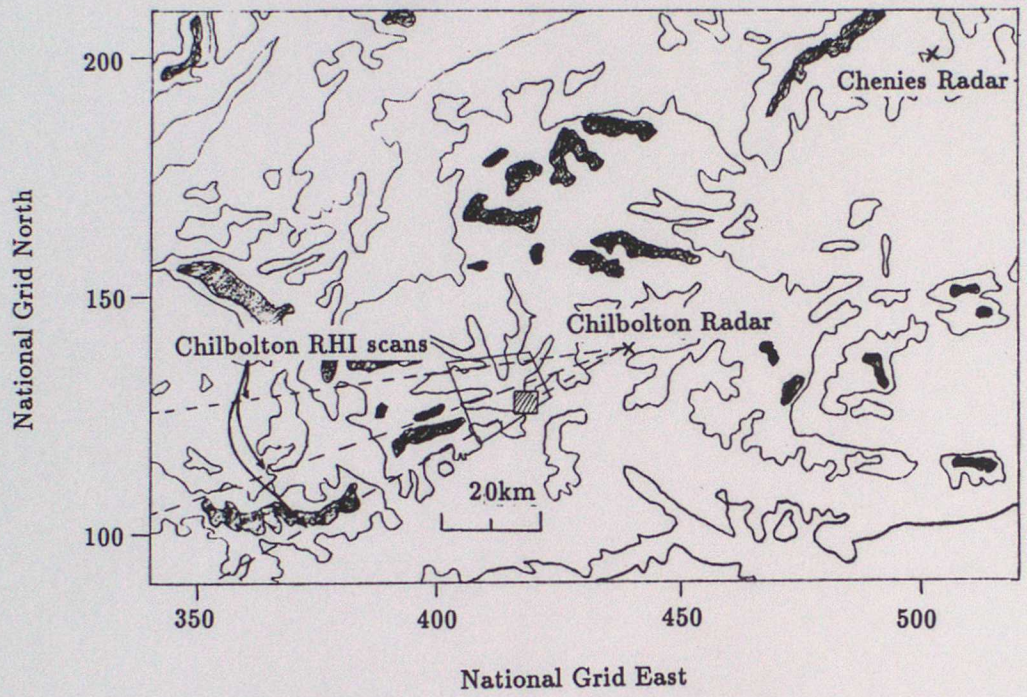

Fig 1

Map of central southern England showing the locations of the two principle radars used in the study. Data from Chilbolton RHI scans within the delineated sector were used to construct the vertical profiles of reflectivity. In the direct comparison experiment, Chilbolton and Chenies data within the shaded box were compared. The 100m contour is shown and the shading denotes ground more than 200m AMSL.

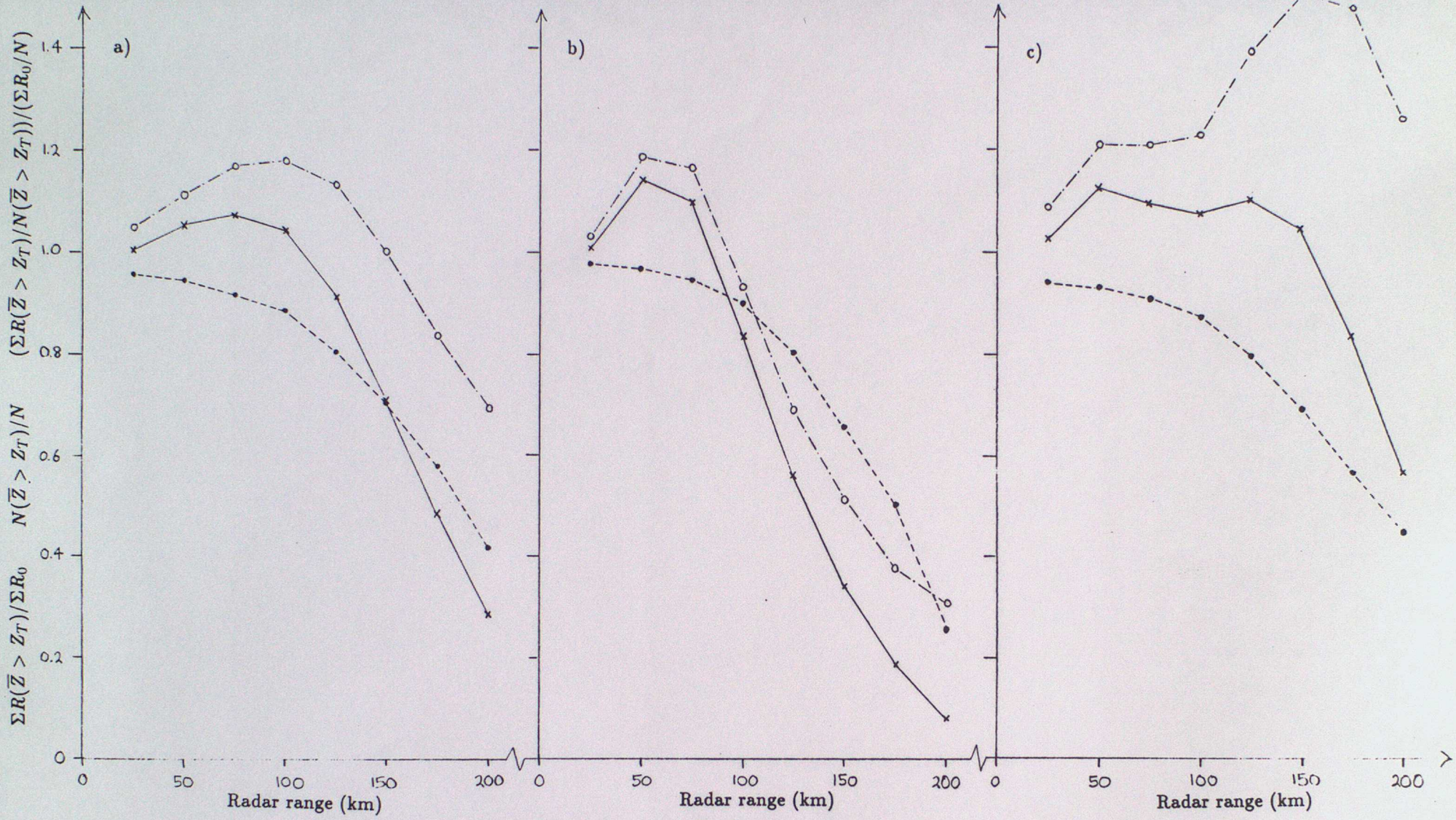

Fig 2

Results of simulations of operational radar performance (assuming a radar height of 100m AMSL and a 0.5 degree elevation beam) based on Chilbolton data. a) is based upon the entire dataset (14440 profiles), b) is for the winter months January-March only (2617 profiles) and c) is for the summer months June-August (2923 profiles). The three quantities plotted as a function of radar range are as follows:-

crosses - $\Sigma R(\overline{Z} > Z_T)/\Sigma R_0$

closed circles - $N(\overline{Z} > Z_T)/N$

open circles - $(\Sigma R(\overline{Z} > Z_T)/N(\overline{Z} > Z_T))/(\Sigma R_0/N)$

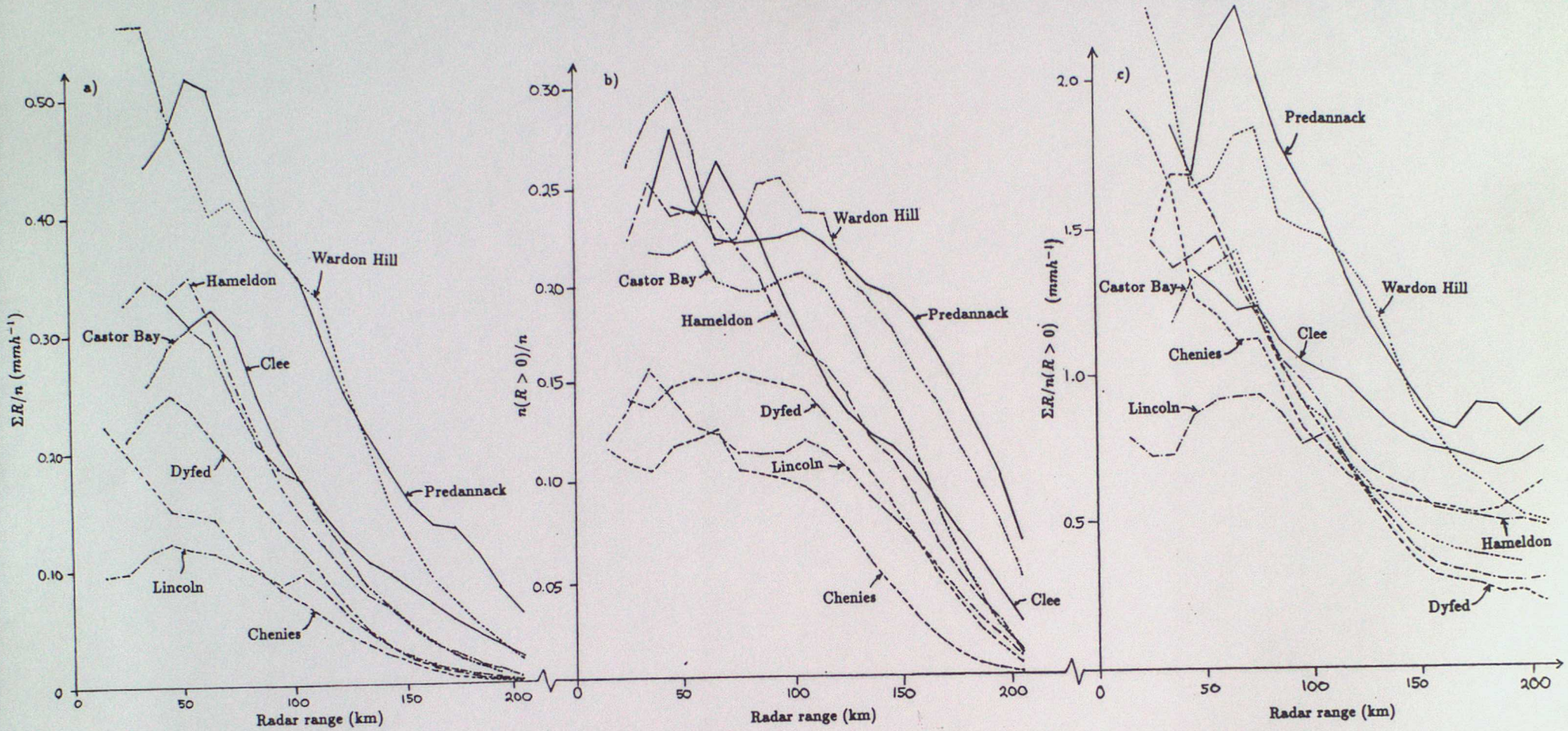

Fig 3

Results of the analysis of data from 8 operational radars for February 1990. The three quantities plotted as a function of radar range are:-

a) The mean rainfall rate within each range band.

b) The fraction of 'wet' pixels.

c) The average rainfall rate for 'wet' pixels.

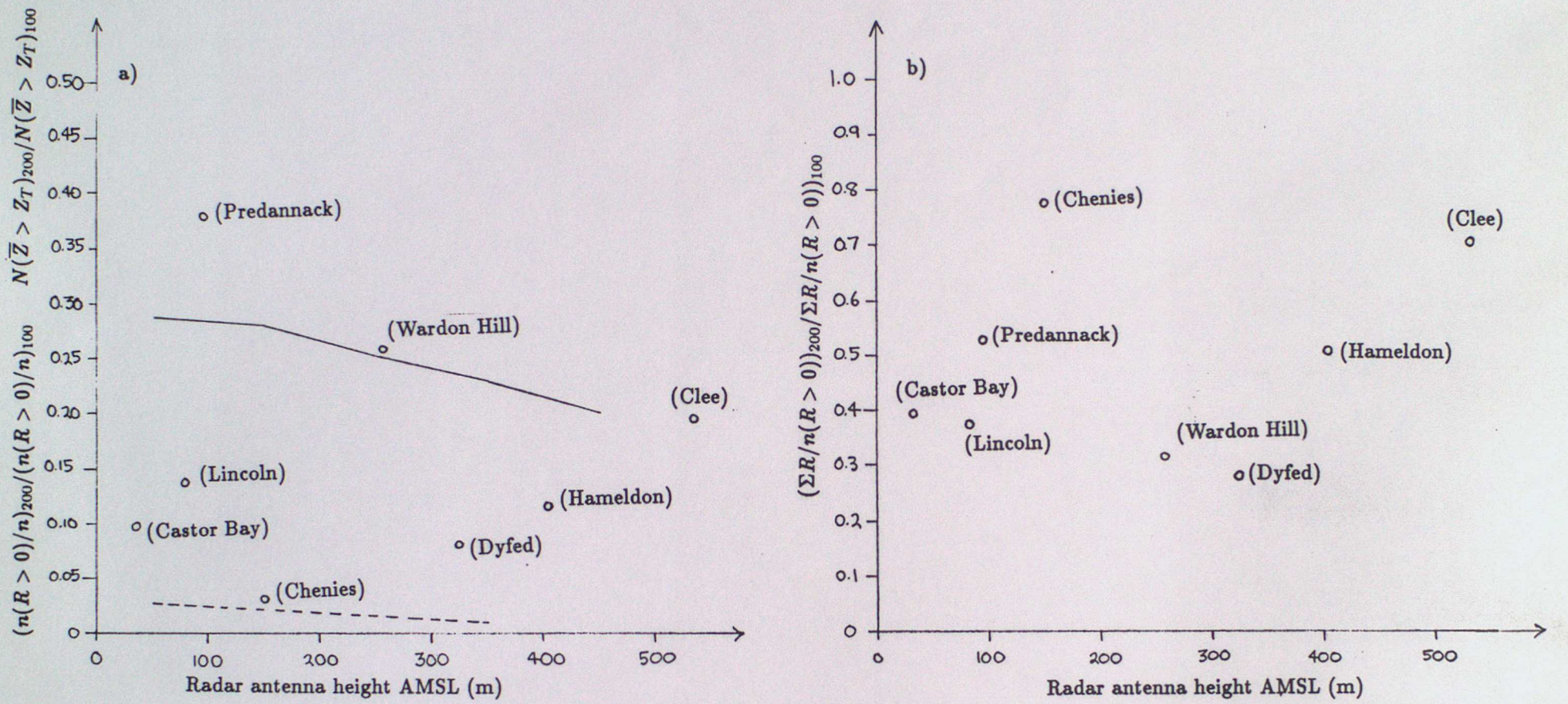

Fig 4

a) The ratios $(n(R>0)/n)_{200}/(n(R>0)/n)_{100}$ (measured) and $N(\overline{Z}>Z_T)_{200}/N(\overline{Z}>Z_T)_{100}$ (simulated) plotted as a function of the radar antenna height. The solid line are the results of simulations with a detection threshold of $0.125mmh^{-1}$ at ranges $\leq 100km$ and the dashed line for a threshold of $0.44mmh^{-1}$ The open circles are the results from the named radars. Note that all the simulations are for a radar beam at 0.5 degrees elevation, the same as that used by all the radars at these ranges except for Clee, whose beam is at 0.0 deg elevation.

b) Values of the ratio $(\Sigma R/n(R>0))_{200}/\Sigma R/n(R>0))_{100}$ for the operational radars plotted as a function of antenna height.

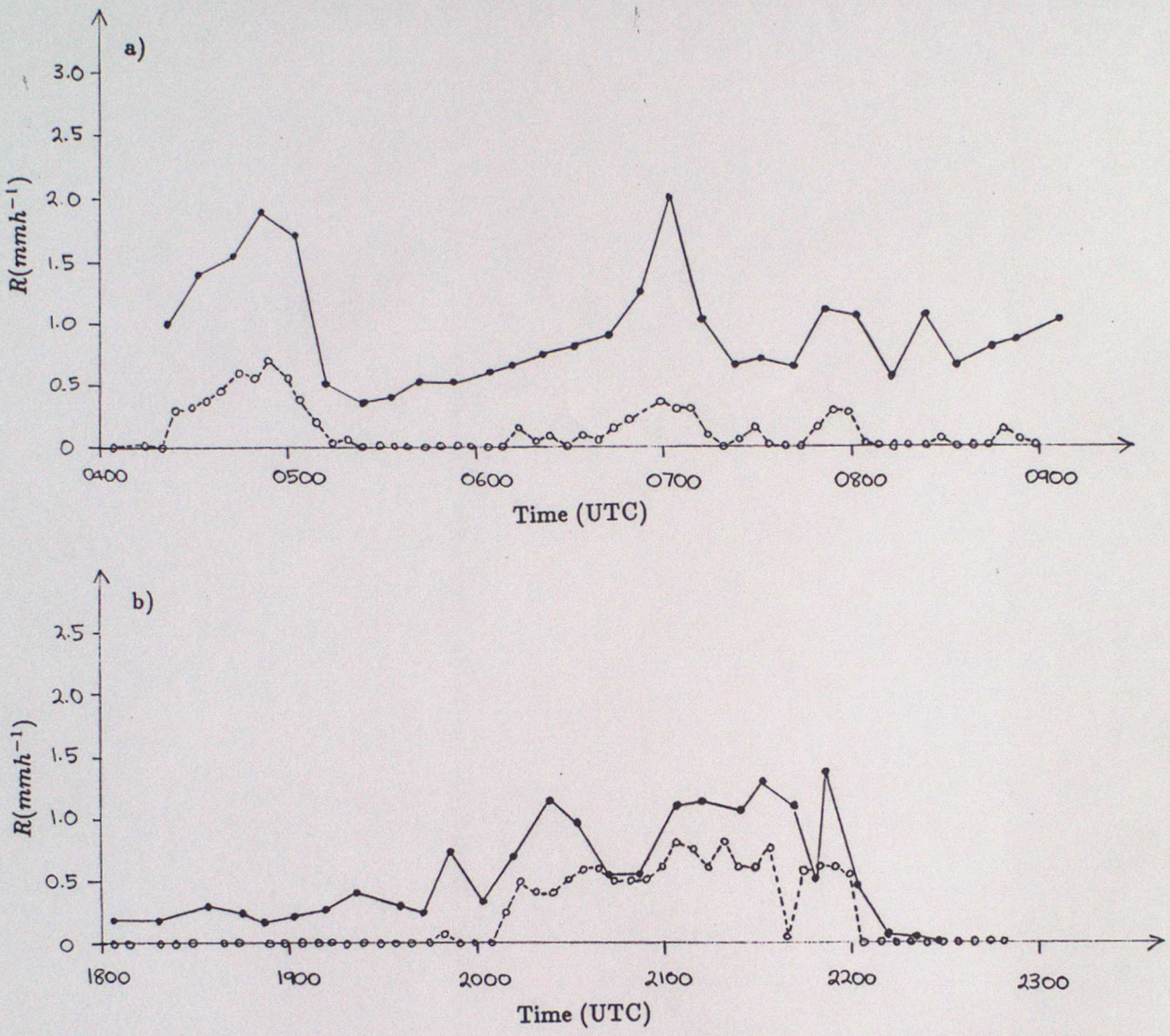

Fig 5

Examples of a time series of Chenies measurements from beam elevation angle 1.5 degrees in a pixel to the SW of the Chilbolton radar (open circles) and simulations of the Chenies measurements from Chilbolton RHI data from within the same pixel (closed circles). a) 0400-0900UTC, 10th Oct 1987, b) 1800-2200UTC 20th Oct 1989.

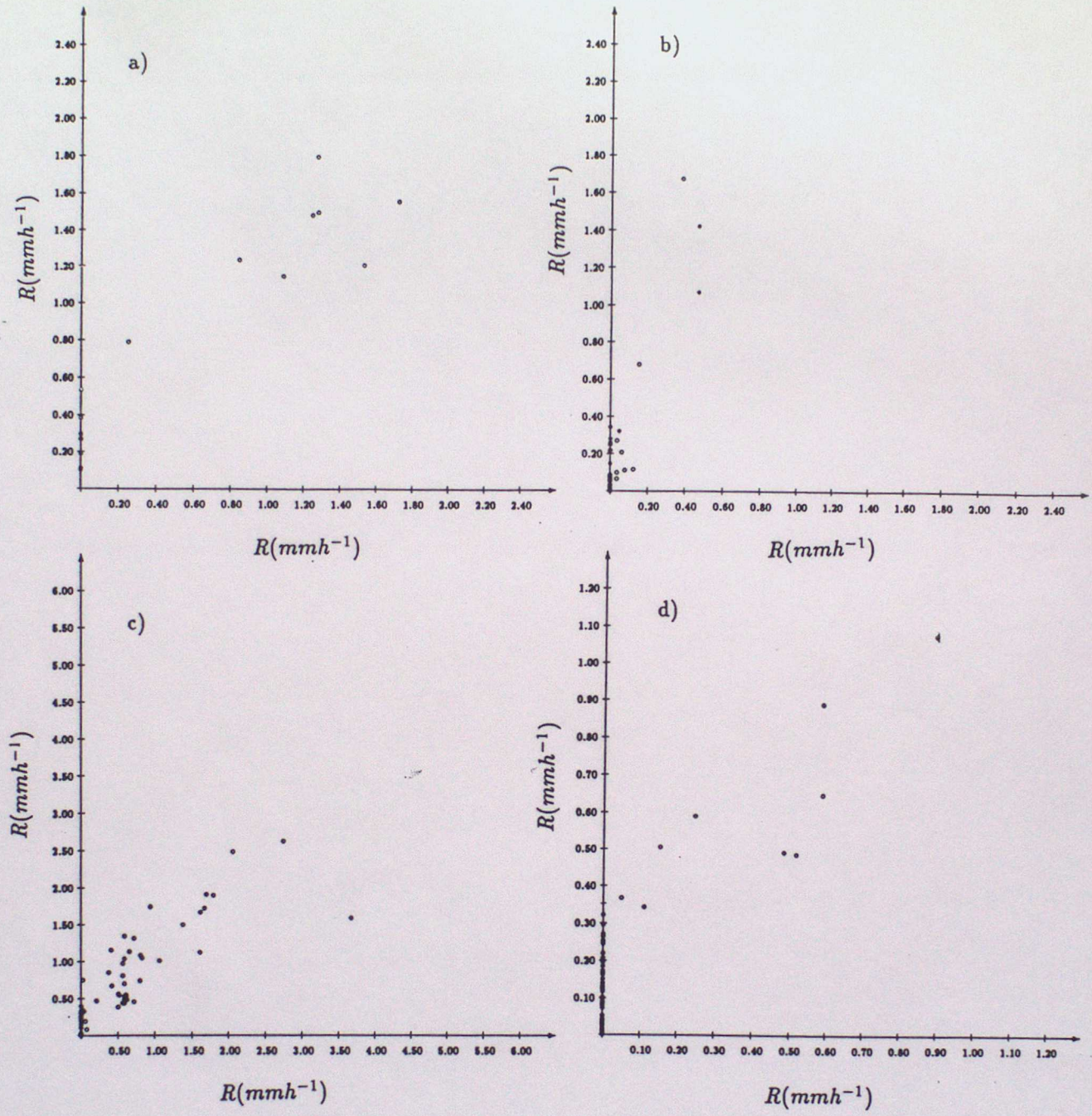

Fig 6

Rainfall rates measured by the Chenies radar (x-axes) compared with simulations from the Chilbolton reflectivity profiles (y-axes).

a) 11 Nov 1987, open circles - Chenies beam elevation 0.5 deg, closed circles - beam elevation 1.5 deg.

b) 28 Sep 1987, open circles - Chenies beam elevation 1.5 deg, closed circles - beam elevation 2.5 deg.

c) 19 Oct 1989, open circles - Chenies beam elevation 1.5 deg.

d) 19 Oct 1989, open circles - Chenies beam elevation 2.5 deg.

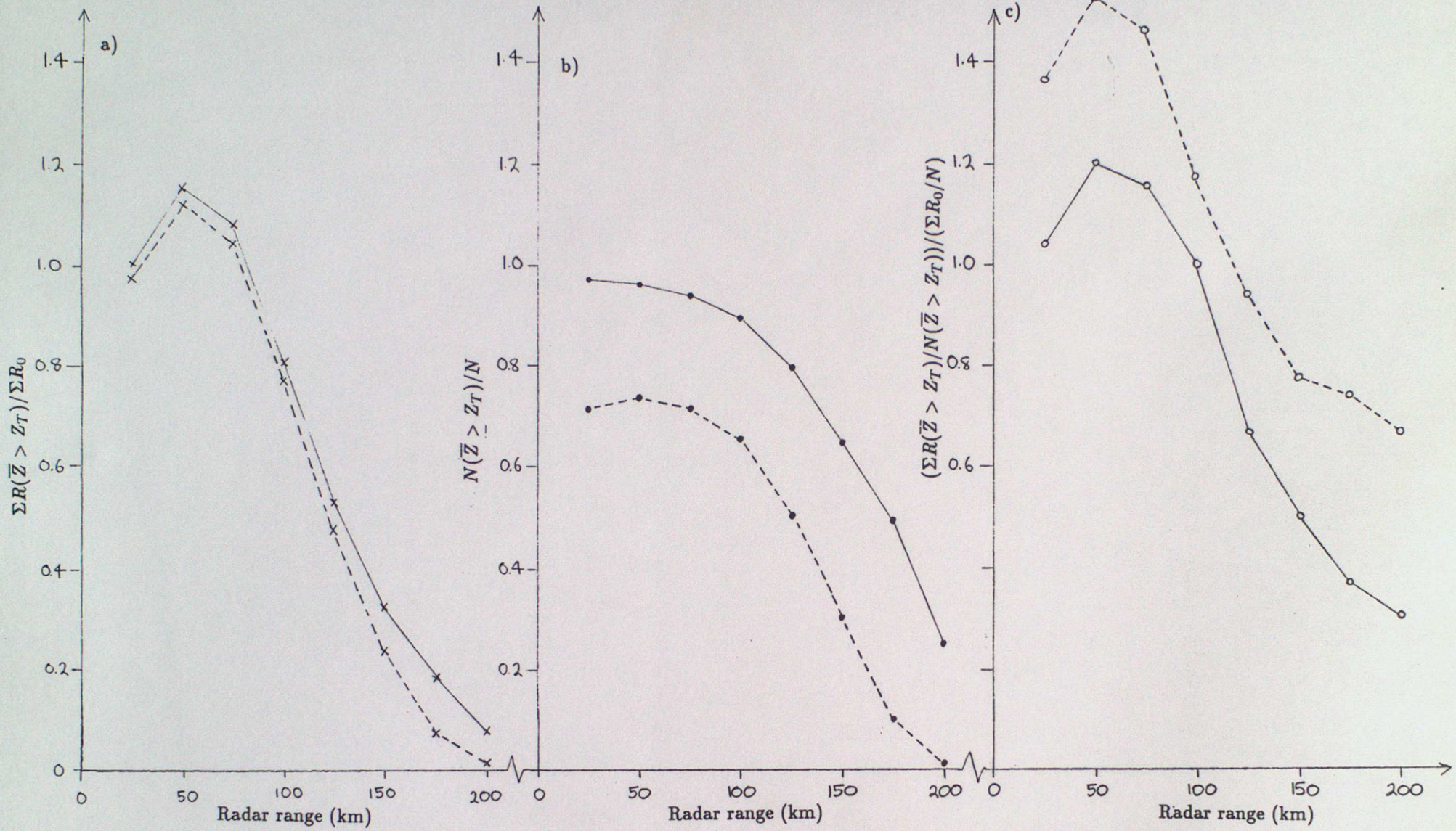

Fig 7

Simulation of Chenies radar performance as a function of range in winter using the Chilbolton reflectivity profiles. The solid lines are for the specification detection threshold and the dashed lines are for the higher thresholds as suggested by the direct comparison experiments. a) the measured rainfall accumulation divided by the surface rainfall accumulation. b) the probability of detection. c) the measured average rainfall rate divided by the average surface rainfall rate.